REVISTA INTERDISCIPLINAR DE PESQUISA EM ENGENHARIA

CILAMCE 2016

XXXVII IBERIAN LATIN AMERICAN CONGRESS ON COMPUTATIONAL METHODS IN ENGINEERING
BRASÍLIA - DF - BRAZIL

DYNAMICS ANALYSIS OF 1D STRUCTURE INCLUDING RANDOM PARAMETER VIA FREQUENCY-DOMAIN STATE-VECTOR EQUATIONS

Marcela Rodrigues Machado

marcelam@unb.br

University of Brasília

Engineering Mechanics Department - Bloco G Sala 1-19/8, 70910-900, Distrito Federal, Brasília, Brazil.

Vilson Souza Pereira, Dalmo I. G. Costa, Elson C. Moraes

vilson.sp@ufma.br

dalmo.costa@ufma.br

elson.cm@ufma.br

Federal University of Maranhão

Mechanical Engineering Course - Avenida dos Portugueses, 1966 ? Bacanga, 65080-805, Maranhão, So Luís, Brazil.

José Maria Campos Dos Santos

zema@fem.unicamp.br

State University of Campinas

Computational Mechanics Department, Faculty of Mechanical Engineering, State University of Campinas-UNICAMP, 13083-970,São Paulo, Campinas, Brazil.

Abstract. *The consideration of uncertainties in numerical models to obtain the probabilistic descriptions of dynamic response is becoming more desirable in the way to quantify the parametric and non-parametric uncertainties associated with the model. In this work, an alternative approach to the spectral element formulation, in which the exact wave solutions are not required,*

the spectral element matrix including random parameters is derived from the transfer matrix formulated directly from the frequency-domain state-vector equation of motion. The analyses were made to quantify the effect of uncertainty in the dynamic responses at high frequency bands and the Monte Carlo simulation is used to propagate the variation in dimensional properties of the structural parameters. Some interesting results are presented, showing the effects of uncertainty parameters in the dynamic response of the structure.

Keywords: *Uncertainty quantification, Transfer matrix, State-Vector, Monte Carlo simulation, Spectral element method.*

1 INTRODUCTION

Modern industry has continually researching new engineering tools, in order to further improve safety and quality of human life. This challenge has led engineers to face constantly new obstacles. In the field of structural dynamics, the purpose is to lower human interaction when monitoring the integrity of a structure. In order to solve this problem, many researchers have made significant progress in developing methods to investigate the dynamic behaviour of structures as rods, beams, plates, etc. Another point is the crash resistance of a structure, that depends, in part, on its capacity to propagate vibrational energy away from the crash site (Doyle, 1997). To study this properly, an itemized analysis of the local behaviour is necessary. It is a preliminary hop towards the analysis of vibration energy propagation in solids. Although frequency domain techniques are efficient and accurate for low frequency band analysis, for high frequency band analysis the solutions are computationally intensive and often provide more information than needed. At high frequency bands structural and acoustic modal parameters (frequency and mode shapes) becomes very dense and impossible to analyse like in low frequency bands. Then, to use theses result as statistical (average) instead of a deterministic is more simple and useful for the engineers. These characteristics of classical solutions have led many researchers to explore new methods to modelling the response of dynamic systems at a less exact result that gives an average overall behaviour of the system. A vast amount of research has been dedicated to the high-frequency range, and one of the techniques most commonly used is statistical energy analysis (SEA) (Lyon and DeJong, 1975). Its limitation comes from the inability to calculate the energy spatial variation in each subsystem. Wohlever (J.C. Wohlever, 1992) proposed the the energy flow analysis (EFA) which is an enhanced of SEA, since it provides the spatial energy distribution within the subsystems. Based on this two techniques combined with the spectral element method (SEM) Doyle (1997); Lee (2004), Santos et al. (Santos et al., 2008) proposed the energy spectral element method (ESEM), which consists of applying the same matrix methodology of FEM to the analytical solution of EFA . Proposed by Lee (Lee, 2000, 2004) the spectral transfer matrix method use the spectral element matrix computed numerically directly from the transfer (or transition) matrix formulated from the state vector equation of motion of a structure. The transfer matrix method (TMM) can be efficiently used especially for periodic one-dimensional structures and can also be applied to energy-based methods.

In the present literature, SEM also TMM do not account in their formulation the presence of uncertainties, like to the geometric parameters, material properties and boundary conditions among others. In the last decades dynamic structure studies have been including this uncertainty information in the models. The Direct Method consists in applying the moment equations to obtain the random solutions. Unknowns are the moments and their equations are derived by taking averages over the original stochastic governing equations. Otherwise, non-sampling approaches may be used, such as the Perturbation method (Kleiber and Hien, 1992; Xiu, 2010), Neumann expansion method (Yamazaki et al., 1988; Zhu et al., 1992), Moment Equations (Xiu, 2010), Polynomial Chaos (PC) expansion and Generalized Polynomial Chaos (Ghanem and Spanos, 1991; Xiu, 2010), Stochastic Galerkin method (Maître and Knio, 2010), Stochastic Partial Differential Equations (SPDEs), and Stochastic Finite Element method (Ghanem and Spanos, 1991). Due to the simple process and high precision, Monte Carlo (MC) simulation has been widely used in probability and statistics analysis; MC also describes the uncertainty propagation of the input/output variables Sobol' (1994).

In this work the dynamic behaviour of a simple rod (elementary rod theory) and a beam element (Euler-Bernoulli theory) is analysed through the perspective of longitudinal and flexural wave propagation and considering the presence of uncertainties in axial rigidity, flexural rigidity and mass per unit of length. This goal is achieved by using an spectral element formulation derived from the transfer matrix formulated as a state vector equation of motion Lee (2000) including the random parameter in the formulation. In additional, a study involving a state vector equation spectrally formulated calculated by TMM is demonstrated and applied to calculate the structural energy density and flow. Analyses were based on quantifying the effect of uncertainty in the dynamic responses at the frequency band of interest. Some interesting results show the effects of uncertainty parameters in the dynamic response of the structure.

2 STATE-VECTOR EQUATION BASED ON SPECTRAL ELEMENT FORMULATION

The spectral elements are formulated by the exact shape functions derived from the wave solutions of a structural model Doyle (1997). In this section, it will be shown that the spectral element matrix can be derived from the transfer matrix spectrally formulated directly from a state vector equation of motion. From dynamic system relationship a frequency-domain state-vector equation can be obtained as,

$$\frac{d\hat{\mathbf{y}}}{dx} = \mathbf{A}(\omega)\hat{\mathbf{y}} \qquad (0 \leq x \leq L) \tag{1}$$

where $\mathbf{A}(\omega)$ is the system matrix and $\hat{\mathbf{y}}(x)$ is the state vector. For a structural system $\hat{\mathbf{y}}(x) = \{\hat{\mathbf{d}} \quad \hat{\mathbf{F}}\}^T$, where $\hat{\mathbf{d}}$ is the nodal displacements vector and $\hat{\mathbf{F}}$ is the internal nodal forces vector.

The general solution of Eq. (1) is given by

$$\hat{\mathbf{y}}(L) = e^{\mathbf{A}L}\hat{\mathbf{y}}(0) = \underbrace{\begin{bmatrix} T_{11} & T_{12} \\ T_{21} & T_{22} \end{bmatrix}}_{\mathbf{T}} \hat{\mathbf{y}}(0) \tag{2}$$

where $\mathbf{T}$ is the transfer matrix, which relates the state vector in the input side $(x = 0)$ to those in the output side $(x = L)$. By rearranging Eq. (2) into the force-displacement formulation based on a two-node element it has,

$$\begin{Bmatrix} \hat{F}_1 \\ \hat{F}_2 \end{Bmatrix} = \begin{bmatrix} T_{12}^{-1}T_{11} & -T_{12}^{-1} \\ T_{21} - T_{22}T_{12}^{-1}T_{11} & T_{22}T_{12}^{-1} \end{bmatrix} \begin{Bmatrix} \hat{d}_1 \\ \hat{d}_2 \end{Bmatrix} \tag{3}$$

or, in a matrix form

$$\{\hat{\mathbf{F}}\} = [\mathbf{S}(\omega)]\,\{\hat{\mathbf{d}}\} \tag{4}$$

where $\mathbf{S}(\omega)$ is the spectral element matrix. This approach does not require a previous knowledge of the wave solutions or the exact shape functions for the problem.

2.1 Rod model with random parameter

The elementary theory considers that the rod is a long and thin structure. Also, it assumes that the axial deformation along the neutral axis of the rod are the same throughout the cross section and the lateral contraction (Poisson effect) can be neglected. The frequency domain homogeneous undamped rod equation of motion is given by:

$$EA(\theta)\frac{\partial^2 \hat{u}(x,\theta)}{\partial x^2} - \omega^2 \rho A(\theta)\hat{u}(x,\theta) = 0 \tag{5}$$

where A is the cross-section area, ρ is the volume mass density, EA is the longitudinal rigidity, ρA is the mass per unit length, u is the longitudinal displacement, ω is the circular frequency, and θ denotes random variable statement. The elastic wave characteristics within a rod element with longitudinal rigidity and mass per unit length are considered as random variable. A hysteretic structural damping is assumed and introduced into the formulation by adding a complex damping factor in the Young's modulus. In the deterministic case it is a complex value given by $E = E_0(1 + i\eta)$, where E_0 is the Young's modulus mean value, η is the damping factor and $i = \sqrt{-1}$ (Doyle, 1997). In the stochastic case it is given by $E(\theta) = \hat{E}(\theta) + E_0 i\eta$, where the random part of the Young's modulus is a real value, $\hat{E}(\theta)$, and the deterministic part is the complex value $E_0 i\eta$.

The rod element state vector in its spectral form is given by

$$\hat{\mathbf{y}}(x,\theta) = \left\{ \begin{array}{c} \hat{d} \\ \hat{F} \end{array} \right\} = \left\{ \begin{array}{c} \hat{u}(x,\theta) \\ EA(\theta)\hat{u}'(x,\theta) \end{array} \right\} \tag{6}$$

where $\hat{d}$ and $\hat{F}$ are the spectral components of the longitudinal displacement and axial force, respectively. Consider a clamped-free rod excited by a harmonic punctual force as show in Fig. (1). Then, Eq. (5) can be transformed into the state-vector form given by Eq. (1) to obtain,

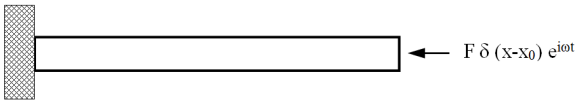

Figure 1: Clamped-free rod with external load.

$$\mathbf{A}(\omega,\theta) = \left[\begin{array}{cc} 0 & 1/EA(\theta) \\ -EA(\theta)k^2 & 0 \end{array} \right] \tag{7}$$

where $k = \omega\sqrt{\rho A(\theta)/EA(\theta)}$ is the rod wavenumber. Since the exponential of system matrix (Eq. 7) can be expressed in closed form, it has

$$e^{\mathbf{A}(\omega,\theta)x} = \left[\begin{array}{cc} \cos(kx) & \frac{1}{kEA(\theta)}\sin(kx) \\ -kEA(\theta)\sin(kx) & cos(kx) \end{array} \right] \tag{8}$$

The transfer matrix for rod member $\mathbf{T}$ can be readily derived as

$$\mathbf{T} = e^{\mathbf{A}(\omega,\theta)L} = \begin{bmatrix} \cos(kL) & \frac{1}{kEA(\theta)}\sin(kL) \\ -kEA(\theta)\sin(kL) & cos(kL) \end{bmatrix} \tag{9}$$

and the state vector of motion for a finite rod element with length L will be

$$\hat{\mathbf{y}}(x,\theta) = \begin{Bmatrix} \hat{d} \\ \hat{F} \end{Bmatrix} = \begin{Bmatrix} F\sec(kL)\sin(x)/(kEA(\theta)) \\ F\cos(kx)\sec(kL) \end{Bmatrix} \tag{10}$$

From the spectral state-vector element (Eq. 10) the longitudinal displacement are obtained and used to calculate rod element energy density and energy flow. The energy density for longitudinal waves in a rod can be written as time-average of instantaneous potential plus kinetic energy densities (Kinsler et al., 1982) to obtain,

$$\langle e \rangle (x,\theta) = \frac{\rho A(\theta)\omega^2}{4}\left\{\hat{u}(x,\theta)\hat{u}(x,\theta)^*\right\} + \frac{EA(\theta)}{4}\left\{\frac{d\hat{u}(x,\theta)}{dx}\frac{d\hat{u}(x,\theta)}{dx}^*\right\}, \tag{11}$$

where $\langle \bullet \rangle$ and $*$ represent the time-averaged quantity and the complex conjugate, respectively. The energy flow for longitudinal waves in a rod can be written as time-average of half of the real part of input axial force times conjugate of longitudinal velocity (Cho and Bernhard, 1998), than it has

$$\langle q \rangle (\theta) = \frac{1}{2}\Re\left\{-i\omega EA(\theta)\frac{d\hat{u}(x,\theta)}{dx}\hat{u}(x,\theta)^*\right\}. \tag{12}$$

2.2 Beam model with random parameter

The undamped governing equation with random flexural rigidity (EI) and mass per unit of length (ρA) for the Euler-Bernoulli beam model (Lee, 2000) is given by

$$EI(\theta)\frac{\partial^4\hat{u}}{\partial x^4} - \omega^2\rho A(\theta)\hat{u} = 0 \tag{13}$$

It can be transformed into four first-order ordinary differential equations, which provides a state-vector equation similar to Eq. (1) but with

$$\hat{\mathbf{y}}(x,\theta) = \begin{Bmatrix} \hat{\mathbf{d}}_B \\ \hat{\mathbf{F}}_B \end{Bmatrix} = \begin{Bmatrix} \hat{v}(x,\theta) \\ \hat{\phi}(x,\theta) \\ -EI(\theta)\hat{v}'''(x,\theta) \\ EI(\theta)\hat{v}''(x,\theta) \end{Bmatrix} \tag{14}$$

where $\hat{v}$ and $\hat{\phi} = \hat{v}'$ are the spectral components of vertical displacement and slope, respectively. Consider a clamped-free beam exited by a harmonic punctual transverse force as show in Fig. (2).

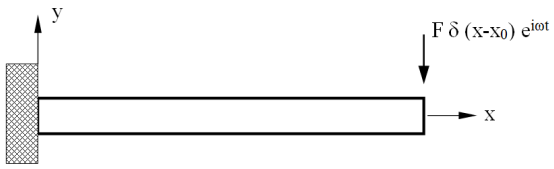

Figure 2: Beam clamped-free and external load.

The matrix $\mathbf{A}(\omega,\theta)$ of the state vector Eq. (1) is derived as

$$\mathbf{A}(\omega,\theta) = \begin{bmatrix} 0 & 1 & 0 & 0 \\ 0 & 0 & 0 & 1/EI \\ -EIk_B^4 & 0 & 0 & 0 \\ 0 & 0 & -1 & 0 \end{bmatrix} \tag{15}$$

where $k_B = \sqrt{\omega}[\rho A(\theta)/EA(\theta)]^{1/4}$ is the beam wavenumber. The spectral transfer matrix can be obtained as

$$e^{\mathbf{A}(\omega,\theta)L} = \mathbf{T} = \begin{bmatrix} T_{11} & T_{12} \\ T_{21} & T_{22} \end{bmatrix}, \tag{16}$$

where the sub-matrices T_{ij} are given by

$$T_{11} = \frac{1}{2}\begin{bmatrix} \cos(kL)+\cosh(kL) & k(\sin(kL)+\sinh(kL)) \\ k(\sinh(kL)-\sin(kL)) & \cos(kL)+\cosh(kL) \end{bmatrix},$$

$$T_{12} = \frac{1}{2EIk^3}\begin{bmatrix} \sin(kL)-\sinh(kL) & \cosh(kL)-\cos(kL) \\ \cos(kL)-\cosh(kL) & \sin(kL)+\sinh(kL) \end{bmatrix},$$

$$T_{21} = \frac{EI}{2}\begin{bmatrix} -k^3(\sin(kL)+\sinh(kL)) & k^2(\cos(kL)-\cosh(kL)) \\ k^2(\cosh(kL)-\cos(kL)) & k(\sinh(kL)-\sin(kL)) \end{bmatrix},$$

$$T_{22} = \frac{1}{2}\begin{bmatrix} \cos(kL)+\cosh(kL) & k(\sin(kL)-\sinh(kL)) \\ -k(\sin(kL)+\sinh(kL)) & \cos(kL)+\cosh(kL) \end{bmatrix} \tag{17}$$

The closed-form solution of state vector of motion (Eq. 14) for a finite beam element of length L is

$$\hat{\mathbf{y}}(x,\theta) \;=\; \begin{Bmatrix} \hat{\mathbf{d}}_B \\ \hat{\mathbf{F}}_B \end{Bmatrix} = \tag{18}$$

$$\left\{\begin{array}{c} \frac{F(\sin(k(L-x))-\sinh(k(L-x))+\sinh(kL)\cos(kx)+\cos(kL)\sinh(kx)+\sin(kL)(-\cosh(kx))-\cosh(kL)\sin(kx))}{2EIk^3(\cos(kL)\cosh(kL)+1)} \\ -\frac{F(\cos(k(L-x))+\sinh(kL)\sin(kx)+\sinh(kx)(\sin(kL)+\sinh(kL))+\cosh(kL)(\cos(kx)-\cosh(kx))-\cos(kL)\cosh(kx))}{2EIk^2(\cos(kL)\cosh(kL)+1)} \\ -\frac{F(\cos(k(L-x))+\cosh(k(L-x))+\sinh(kL)\sin(kx)-\sin(kL)\sinh(kx)+\cosh(kL)\cos(kx)+\cos(kL)\cosh(kx))}{2\cos(kL)\cosh(kL)+2} \\ -\frac{F(\sin(k(L-x))+\sinh(k(L-x))+\sinh(kL)\cos(kx)-\cos(kL)\sinh(kx)+\sin(kL)\cosh(kx)-\cosh(kL)\sin(kx))}{2(k\cos(kL)\cosh(kL)+k)} \end{array}\right\}$$

Similarly to rod model the energy analysis is performed to beam model. From the Euler-Bernoulli beam model the flexural displacements are obtained (Eq. 18) and used to calculate energy density and energy flow. For a harmonic excitation, the time-averaged energy density and flow due to flexural waves can be written as (Cho and Bernhard, 1998),

$$\langle e\rangle_F(x,\theta) = \frac{\rho A(\theta)\omega^2}{4}\left\{\hat{v}(x,\theta)\hat{v}(x,\theta)^*\right\} + \frac{EI(\theta)}{4}\left\{\frac{d\hat{v}(x,\theta)}{dx}\frac{d\hat{v}(x,\theta)}{dx}^*\right\}, \tag{19}$$

and

$$\langle q\rangle_F(x,\theta) = \frac{1}{2}\Re\left\{-i\omega EI\left(\frac{d^3\hat{v}(x,\theta)}{dx^3}\hat{v}(x,\theta)^* - \frac{d^2\hat{v}(x,\theta)}{dx^2}\frac{d\hat{v}^*(x,\theta)}{dx}\right)\right\}. \tag{20}$$

3 MONTE CARLO SIMULATION

The Monte Carlo simulation has been used for decades, it is a method based on random samples used in approximations. The name itself is taken from the famous casino located in Monte Carlo Sampaio and Lima (2012). Simulation methods are also named exact methods, because the simulation result leads to exact outcomes when the sample number goes to infinity. To avoid certain approximations which occur in analytical methods and to be a non-intrusive method are another advantages of this type of techniques. Thus, the general idea of the method is solving mathematical problems by the simulation of random variables Sobol' (1994). An Monte Carlo method example of application is the multidimensional integral approximation. Supposing the integral of a given real multidimensional function g in a certain region $B \subset \mathbb{R}$,

$$I = \int_B g(\theta)d(\theta) \tag{21}$$

If g is a simple function, its integral (I) can be calculated easily. However, if g is a difficult function or is defined in a region with complicated contour can does not exist a closed form for (I). In such cases, numerical integration methods must be applied for if approximations for (I), such as the trapeze method, Simpson method and Monte Carlo simulation. Assuming that (I) is a one-dimensional integral, p and function density probability of a random variable θ, rewriting equation (21) it is

$$I = \int_B h(\theta)p(\theta)d(\theta) \tag{22}$$

where $h(\theta) = g(\theta)/p(\mathbf{x})\forall\theta \in B$. The integral I can be interpreted as the expected value of $h(\theta)$, it is:

$$I = \mathbb{E}[h(\theta)] = \int_B h(\theta)p(\theta)d(\theta) \tag{23}$$

Thus, and approximation $(\hat{I})$ for the integral can be expressed as

$$\hat{I} = \sum_{i=1}^{n} h(\theta^i) \tag{24}$$

where $\theta(1), \theta(2), ..., \theta(n)$ are samples of the random vector $\boldsymbol{\Theta}$ with probability density function p.

The mean and the standard deviation of the result are calculated through the samples generated. Let $X(\xi, \omega)$ be the frequency response of the stochastic system calculated for a realization ξ, generated by the Monte Carlo method Rubinstein (2008). The mean-square convergence analysis with respect to independent realizations of the random variable θ, denoted by $\Theta_j(\xi, \omega)$, is carried out studying the function $n_S \mapsto conv(n_S)$ defined by:

$$conv(n_S) = \frac{1}{n_S} \sum_{j=1}^{n_S} \int_B \|\Theta_j(\xi, \omega)\|^2 \, d\omega \tag{25}$$

4 NUMERICAL TESTS

Rod

A numerical example is considered to illustrate the application of the rod spectral state-vector model presented in Section 2.1. A clamped-free simple rod structure with the length $L = 1.2$ m and cross-section area $A = 0.04$ cm^2 is analysed. The rod is made of steel with average material properties: density $\rho = 7860$ kg/m^3 and elastic modulus $E = 210$ GPa. The structural damping coefficients is assumed to be $\eta = 0.01$. The axial rigidity and mass per unit length are assumed to be Log-normal random variable with coefficient of variation (COV) of 2 and 10% of the mean values of the random variables. The response is calculated at the rod free end attributable to a unit harmonic force at the same end.

Figure 3 shows the real part of rod longitudinal displacement response calculated with rod spectral state-vector model using EA and ρA parameters as deterministic and random variables (mean and standard deviation) for COV = 0.02 and COV = 0.1. Results show that for COV

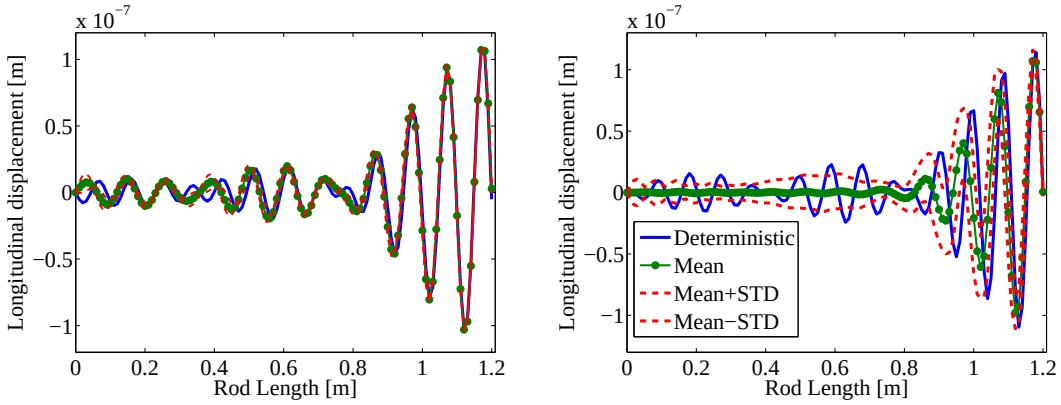

Figure 3: Rod displacement response using deterministic and stochastic (mean and STD envelope) random variables for COV = 2% (LHS) and 10%(RHS).

= 0.02 (Figure 3 LHS) the deterministic and stochastic longitudinal displacement are almost coincident between the excitation/response point ($L = 1.2$ m) and around $L = 0.8$ m. After that position deterministic and mean rod displacement present some mismatches but still very close for the majority of the path along rod length until the left-end. Standard deviation (STD) envelop is coincident also with the other curves. Such behaviour should be expected considering the low variability of random variables. As the coefficient of variation is raised for a more significant value (COV = 0.1) rod displacement deterministic, mean and STD envelop (Figure 3 RHS) are coincident close to the excitation/response point, but presents statistically consistent results for the rest of rod length.

Energy density and flow for rod longitudinal waves are frequency-avareged at 1/3-octave frequency band with centre frequency $f_c = 50$ kHz. Figures Fig. (4) and Fig. (5) show rod energy density and energy flow calculated by Eq. (11) and (12) using deterministic and stochastic mean displacement responses with COV = 0.02 and 0.1.

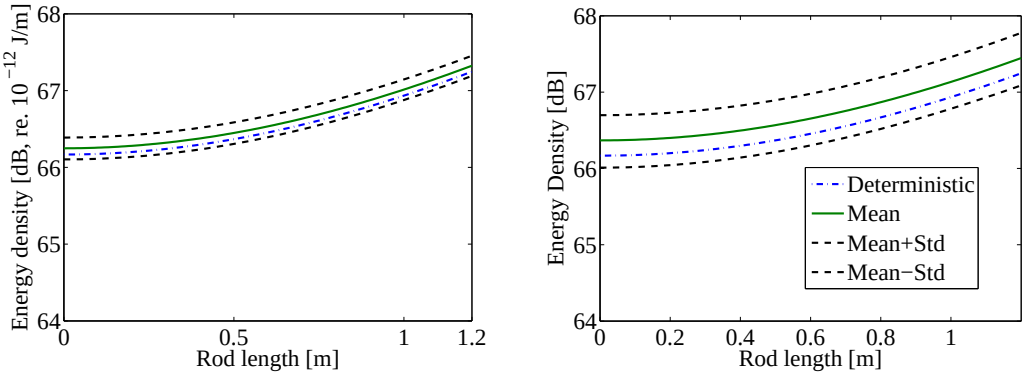

Figure 4: Deterministic, mean and standard deviation envelope rod energy density along the rod ($f_c = 50$ kHz) for COV of 2% (LHS) and 10%(RHS).

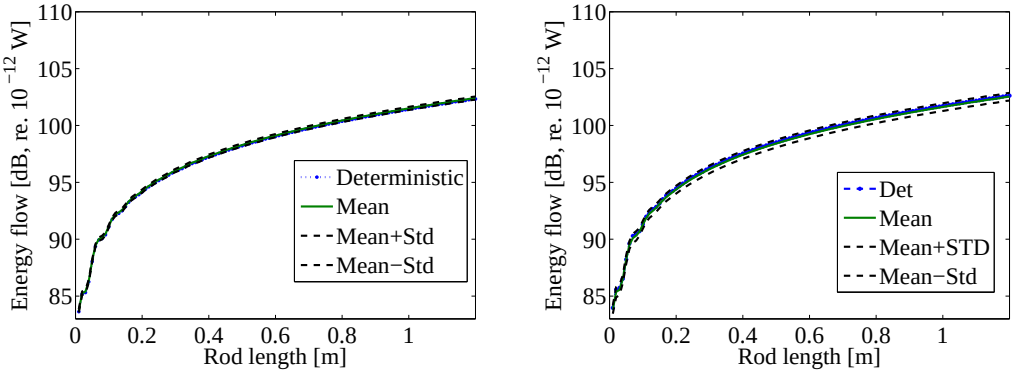

Figure 5: Deterministic, mean and standard deviation envelope rod energy flow along the rod ($f_c = 50$ kHz) for COV of 2% (LHS) and 10%(RHS).

The mean curve is different from the deterministic curve and the standard deviation is biased by the mean. A homogeneous behaviour as for the mean as for the standard deviation envelope is observed along of the rod. These results are obtained by using a Monte Carlo simulation with 1,000 samples which is verify by a convergence analysis (eq. 25) shown in

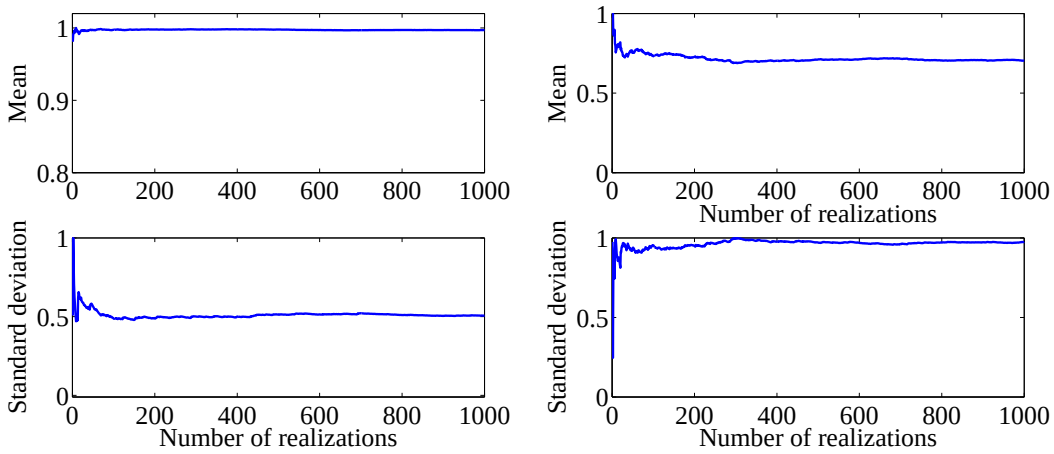

Figure 6: Rod convergence analyse for COV of 2% (LHS) and 10%(RHS).

Fig. (6). For small COV the mean convergence is with around 100 samples, and standard deviation with approximately 300 samples. The mean convergence for COV of 10% is around 350 samples and standard deviation with 500. The computational time used to run the 1000 samples was 20.35 minutes. It was computed by using a Intel(R)Core(TM) i7 CPU @2.20Hz with installed memory (RAM) of 8GB.

Beam

A simple numerical example is considered to illustrate the application of the formulation derived for the Euler-Bernoulli beam. The mean material properties are considered as $\rho = 7860$ kg/m^3 and $E = 210$ GPa. The length of the beam is $L = 2$ m and the rectangular cross section has a width of 20 mm and a thickness of 6 mm. The area moment of inertia of the cross section $I = 1.33^{-9}$ m^4 and the structural damping coefficients are assumed to be $\eta = 0.1$. A clamped- free boundary condition is considered for this example. The standard deviations of both the random fields are assumed to be 2 and 10% of their mean values. We also consider the displacement response at the free end of the beam attributable to a unit harmonic vertical force at that end. The displacement response of the deterministic system, the mean, and the

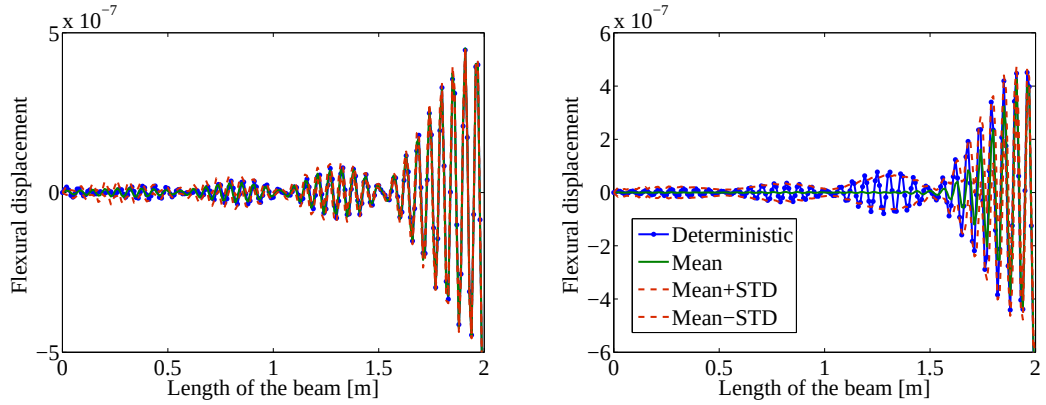

Figure 7: Deterministic, mean and standard deviation envelope beam displacement response along the beam for COV of 2% (LHS) and 10%(RHS).

standard deviation of the real value of the response calculated with eq. (18) are shown in Fig. (7). Similar to rod structure, the mean curve is different from the deterministic curve for the both coefficient of variation (2 and 10%). This difference is larger at higher COV value and as far as the excitation/measured point. Closer to the excitation/measured point, standard deviation is biased by the mean, but as distance as of the point increases, the standard deviation curve flattens.

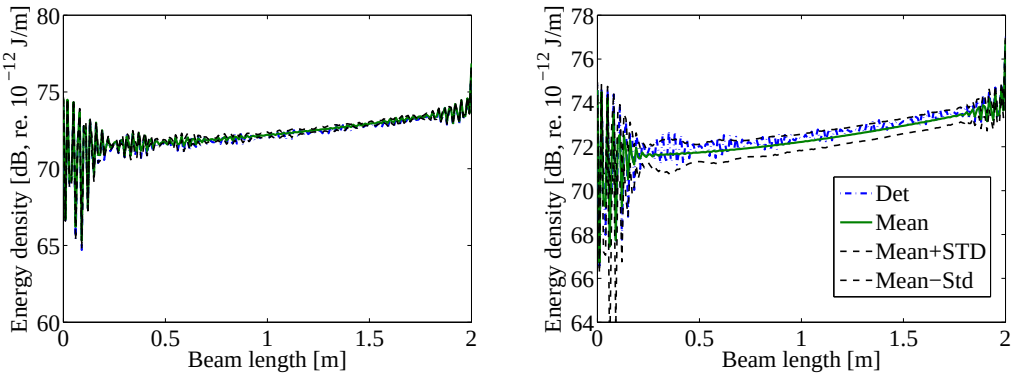

Figure 8: Deterministic, mean and standard deviation envelope beam energy density along the beam ($f_c = 50$ kHz) for COV of 2% (LHS) and 10%(RHS).

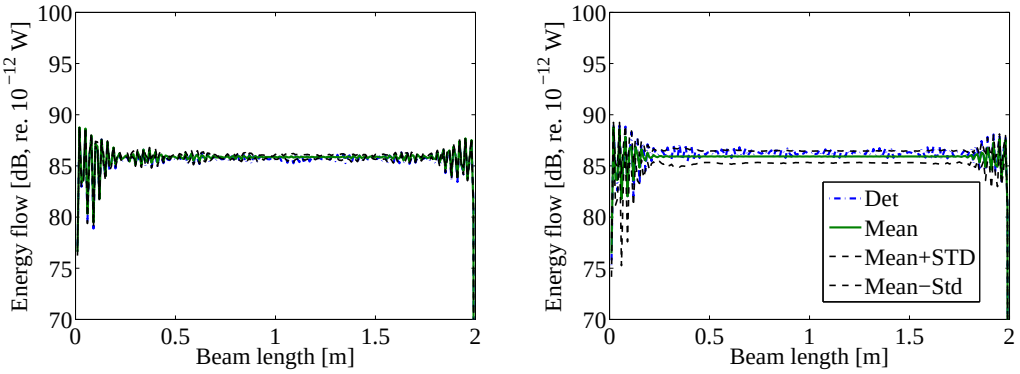

Figure 9: Deterministic, mean and standard deviation envelope beam energy flow along the rod ($f_c = 50$ kHz) for COV of 2% (LHS) and 10%(RHS).

Analysis of the energy density calculated using eq. (19) and energy flow using eq. (20) are shown in Fig. (8) and Fig. (9). They are calculated at 1/3-octave frequency bands with centre frequency $f_c = 50$ kHz. The energies analysis for the beam structure is more sensible than rod, which generates a large difference between mean curve from the deterministic and mean curves, especially for high COV. The standard deviation is biased by the mean. These results are obtained by using a Monte Carlo simulation with 1,000 samples which is also verify by a convergence analysis (eq. 25) shown in Fig. (10). For COV of 2% the mean and standard deviation convergence are with around 200 samples. The mean and standard deviation convergence for COV of 10% are around 800 samples. The computational time used to run the 1000 samples was 24.05 minutes.

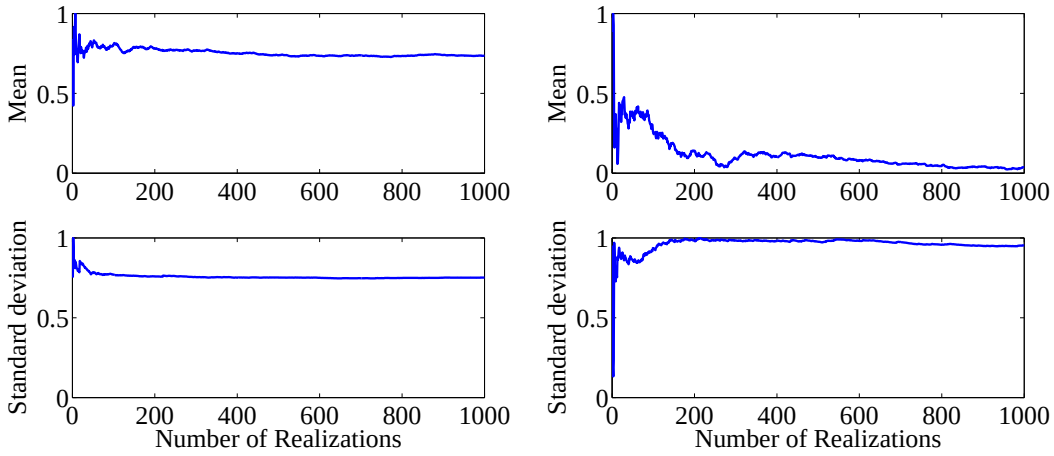

Figure 10: Beam convergence analyse for COV of 2% (LHS) and 10%(RHS).

5 CONCLUSION

The basic formulation for the the spectral transfer matrix method including random parameters were presented. The consideration of uncertainties in numerical models to obtain the probabilistic descriptions of dynamic response turns the analysis more realistic. The analyses were made to quantify the effect of uncertainty in the dynamic responses at high frequencies and use the Monte Carlo simulation to propagate the variation in dimensional properties of the structural parameters. Even for rod as beam, the displacement and energies (density and flow) are calculated at 1/3-octave frequency bands with centre frequency $f_c = 50$ kHz. The displacement response of the deterministic system, the mean, and the standard deviation with COV's of 2 and 10% were demonstrated. In both structures (rod and beam) the mean curve is different from the deterministic curve. This difference is larger at higher COV value and as far as the excitation/measured point. Closer to the excitation/measured point the standard deviation is biased by the mean, as distance of the point increases, the standard deviation curve flattens.

The mean and standard deviation of the energy density and energy flow is homogeneous along the rod. However for beam the energies showed a oscillation because the beam structure is more sensible than the rod. There is a large difference between deterministic and mean curves due to the greater beam sensibility. These results are obtained by using a Monte Carlo simulation with 1,000 samples which is also verified by a convergence analysis. For small COV's the sample number required for a good simulation is smaller than for high COV as demonstrated in this paper. Whole simulations were computed by using a Intel(R)Core(TM) i7 CPU @2.20Hz with installed memory (RAM) of 8GB.

ACKNOWLEDGEMENTS

The authors are grateful to the government research funding agencies Fundação de Apoio à Pesquisa do Estado do Maranhão - FAPEMA, Fundação de Amparo à Pesquisa do Estado de São Paulo - FAPESP, Conselho Nacional de Desenvolvimento Científico e Tecnológico - CNPq and Coordenação de Aperfeiçoamento de Pessoal de Nível Superior - CAPES for the financial support for this work.

REFERENCES

Cho, P. and Bernhard, R. . Energy flow analysis of coupled beams. *Journal of Sound and Vibration*, 211:593–605, 1998.

Doyle, J. F. . *Wave propagation in structures : spectral analysis using fast discrete Fourier transforms*. Mechanical engineering. Springer-Verlag New York, Inc., New York, second edition, 1997.

Ghanem, R. and Spanos, P. . *Stochastic Finite Elements - A Spectral Approach*. Sprin, 1991.

J.C. Wohlever, R. B. . Mechanical energy flow models of rods and beams. *Journal of Sound and Vibration*, 153:1–19, 1992.

Kinsler, L. E. , Frey, A. R. , Coppens, A. B. , and Sanders, J. V. . *Fundamentals of Acoustics*. John Wiley & Sons, 1982.

Kleiber, M. and Hien, T. . *The Stochastic Finite Element Method*. John Wiley, 1992.

Lee, U. . Vibration analysis of one-dimensional structures using the spectral transfer matrix method. *Engineering Structures*, 22(6):681–690, 2000. doi: 10.1016/S0141-0296(99)00002-4.

Lee, U. . *Spectral Element Method in Structural Dynamics*. BInha University Press, 2004.

Lyon, R. H. and DeJong, R. G. . *Theory and Application of Dynamics Systems, Second edition*. Butterworth-Heinemann, Boston, 1975.

Maître, O. L. and Knio, O. . *Spectral methods for uncertainty quantification*. Springer, 2010.

Rubinstein, R. Y. . *Simulation and the Monte Carlo Method, 2nd Edition*. Wiley, 2008.

Sampaio, R. and Lima, R. . *Modelagem Estocástica e Geração de Amostras de Variáveis e Vetores Aleatórios*. SBMAC (Notas em Matemática Aplicada; v. 70), 2012.

Santos, E. , Arruda, J. , and Santos, J. D. . Modeling of coupled structural systems by an energy spectral element method. *Journal of Sound and Vibration*, 36:1 – 24, 2008.

Sobol', I. M. . *A primer for the Monte Carlo method*. CRC Press, 1994.

Xiu, D. . *Numerical Methods for Computations-A Spectral method approcah*. Princeton University Press, 2010.

Yamazaki, F. , Shinozuka, M. , and Dasgupta, G. . Neumann expansion for stochastic finite element analysis. *Journal Engineering Mechanics-ASCE*, 114 (8):1335–1354, 1988.

Zhu, W. , Ren, Y. , and Wu, W. . Stochastic fem based on local averages of random vector fields. *Journal Engineering Mechanics-ASCE*, 118 (3):496–511, 1992.